ResearchGate

See discussions, stats, and author profiles for this publication at: https://www.researchgate.net/publication/295848395

Production, characterization, engine performance and emission characteristics of Croton megalocarpus and Ceiba…

Article *in* RSC Advances · February 2016

DOI: 10.1039/C5RA21750D

CITATIONS
5

READS
104

7 authors, including:



M. A. Kalam
University of Malaya
289 PUBLICATIONS **4,473** CITATIONS
SEE PROFILE



Abdulaziz Atabani (A.E. Atabani)
Erciyes Üniversitesi
52 PUBLICATIONS **1,625** CITATIONS
SEE PROFILE



I. M. Rizwanul Fattah
UNSW Australia
48 PUBLICATIONS **1,000** CITATIONS
SEE PROFILE



M. J. Abedin
Monash University (Australia)
38 PUBLICATIONS **648** CITATIONS
SEE PROFILE

Some of the authors of this publication are also working on these related projects:



Currently I am working on Graphene based nano crystal and nano fiber View project



Frictional Force Analysis for Various Sliding Components of an IC Engine Using Motoring Test Bed View project

All content following this page was uploaded by Abdulaziz Atabani (A.E. Atabani) on 10 March 2016.

The user has requested enhancement of the downloaded file. All in-text references underlined in blue are added to the original document and are linked to publications on ResearchGate, letting you access and read them immediately.

RSC Advances

PAPER

View Article Online
View Journal | View Issue

CrossMark click for updates

Cite this: *RSC Adv.*, 2016, **6**, 24584

Published on 22 February 2016. Downloaded by University of Malaya on 08/03/2016 12:41:13.

Production, characterization, engine performance and emission characteristics of *Croton megalocarpus* and *Ceiba pentandra* complementary blends in a single-cylinder diesel engine

A. M. Ruhul,*[a] M. A. Kalam,[a] H. H. Masjuki,*[a] Abdullah Alabdulkarem,[b] A. E. Atabani,[c] I. M. Rizwanul Fattah[d] and M. J. Abedin[a]

Received 18th October 2015
Accepted 20th February 2016

DOI: 10.1039/c5ra21750d

www.rsc.org/advances

Compounding energy demand and environmental issues necessitate suitable alternative or partial replacement of fossil fuels. Among the possible sources, biodiesel from non-edible vegetable oil sources is more economically feasible and possesses characteristics close to those of petroleum diesel. Two potential non-edible biodiesel feedstocks "*Croton megalocarpus*" and "*Ceiba pentandra*" were used for biodiesel production through esterification and transesterification process on a laboratory scale. Biodiesel characterization, engine performance and emission characteristics were investigated in an unmodified direct injection, naturally aspirated, single-cylinder diesel engine. 20% (v/v) of each of *C. megalocarpus* (CM), *C. pentandra* (CP) and their combined blends (CMB20, CPB20, CMB15CPB05, CMB10CPB10, and CMB05CPB15) were tested under varying engine speeds ranging from 1000 rpm to 2400 rpm at full load conditions. CMB20 and CPB20 reduced the brake power (BP) by 2.63% and 3.70%, brake thermal efficiency (BTE) by 5.97% and 3.72%, carbon monoxide (CO) emission by 1.09% and 2.39%, hydrocarbon (HC) emission by 1.48% and 4.62% and smoke emission by 12.35% and 17.13%, respectively compared to petroleum diesel. On the other hand, CMB20 and CPB20 increased the brake specific fuel consumption (BSFC) by 9.74% and 7.63%, NO_X emission by 13.19% and 15.45%, respectively. A mixture of 10% of both biodiesels with diesels (CMB10CPB10) provides better performance and emission characteristics. CMB10CPB10 reduced BP, BTE, CO, HC and smoke by 0.53%, 0.50%, 5.21%, 8.38% and 20.71%, respectively and increased BSFC and NO_X by 3.90% and 18.66%, respectively compared to conventional diesel. A combined blend of CM and CP could be a sustainable substitute for fossil diesel in the context of performance and emission.

1. Introduction

The consumption of fossil fuels is increasing day by day due to the increase in energy demand worldwide, which results in diminishing fossil fuel reserves. The quick consumption and rising costs of petroleum fuel other than their harmful emission are the primary reasons to look for alternative renewable sources. Thus, research on alternative and renewable energy sources is always a burning issue for future energy demand fulfillment. Biofuel is one of the potential alternative resources. The term biofuel refers to liquid or gaseous fuels that are predominantly produced from biomass. A variety of fuels can be produced from biomass resources including liquid fuels, such as bioethanol, methanol, biodiesel, Fischer–Tropsch diesel, and gaseous fuels, such as hydrogen and methane.[1] Biodiesel is the most convenient alternative source that could play a very important role to meet the energy demand, especially in automobile and power generation sector. Generally, it is synthesized from edible oils due to abundance and low free fatty acid content. Biodiesel contains alkyl ester which could be derived by transesterification of triglycerides or esterification of free fatty acids with lower weight alcohol. On the other hand, the consideration is essentially engaged towards biodiesel from non-edible feedstocks as dependency on edible source pose threat to food supply. In addition, production of biodiesel from non-edible feedstocks decreases the expense of biodiesel as these are

[a]*Centre for Energy Sciences, Department of Mechanical Engineering, Faculty of Engineering, University of Malaya, 50603 Kuala Lumpur, Malaysia. E-mail: ruhulamin07ruet@gmail.com; masjuki@um.edu.my; Fax: +603 79675317; Tel: +603 79674448*

[b]*Mechanical Engineering Department, College of Engineering, King Saud University, 11421 Riyadh, Saudi Arabia*

[c]*Department of Mechanical Engineering, Faculty of Engineering, Erciyes University, 38039 Kayseri, Turkey*

[d]*School of Mechanical and Manufacturing Engineering, University of New South Wales, Kensington, 2052 NSW, Australia*

This journal is © The Royal Society of Chemistry 2016

Published on 22 February 2016. Downloaded by University of Malaya on 08/03/2016 12:41:13.

fundamentally less expensive.[2,3] *Croton megalocarpus* and *Ceiba pentandra* are two of the potential non-edible feedstocks which have recently drawn attention of the researchers.[4–7]

Silitonga *et al.*[4] produced biodiesel from *Ceiba pentandra* feedstock through combined acid esterification and base transesterification process. For acid esterification, 1% (v/v) of H_2SO_4 acid catalyst, 60 °C reaction temperature and 2 h reaction time was used. During base transesterification, 1% (w/w) of NaOH catalyst, 50 °C temperature and 2 h time was used was used. In both cases they have used 8 : 1 methanol to oil molar ratio and 1200 rpm stirring speed. They also characterized different properties of different blends of up to 50% with diesel. Ong *et al.*[8] and Silitonga *et al.*[9] investigated engine performance and emission with up to 50% *C. pentandra* biodiesel blending with diesel in every 10% composition interval. They found that 10% blend provides better results in terms of torque, power, and fuel consumption than other blend ratios. Vedharaj *et al.*[10] obtained 4% superior thermal efficiency than conventional diesel for 25% CPB–diesel blend. Bokhari *et al.*[11] introduced the microwave-assisted technique to optimize the conversion of *C. pentandra* oil using response surface methodology (RSM). They recorded optimized condition of 1 : 9.85 oil to methanol molar ratio, 2.15 wt% KOH catalyst loading, 57.09 °C reaction temperature and 3.29 minute reaction time for 98.9% yield.

Kafuku *et al.*[12] investigated the production optimization and the effects of different parameters of transesterification reaction during converting the methyl ester from *C. megalocarpus*. They varied the catalyst from 0.5 wt% to 1.5 wt% with 0.25 wt% interval, reaction time from 30 minutes to 90 minutes with 15 minute interval, methanol to oil ratio from 10% (w/w) to 50% (w/w) with 10 wt% interval, reaction temperature 30 °C to 60 °C with 10 °C interval, and stirring speed 20 rpm to 800 rpm with 200 rpm interval. They found that 1 wt% catalytic loading, 30 wt% methanol loading and 60 minutes reaction time gives an optimum yield of 90%. Aliyu *et al.*[13] investigated the performance and emission characteristics of *C. megalocarpus* based biodiesel on 4 stroke 3-cylinder unmodified diesel engine. They found lower BTE and higher exhaust temperature for biodiesel blends compare to diesel.

Earlier studies have addressed the suitability of the biodiesel and its blends derived from these feedstocks in diesel engines. However, combined blend of multiple feedstocks are being tested nowadays to improve the biodiesel economics while simultaneously enhancing fuel performance.[14] Habibullah *et al.*[15] studied the effect of 20% (v/v) palm, coconut, palm–coconut (PB5CB15, PB10CB10 and PB15CB5) biodiesel and 30% (v/v)[16] palm, coconut and palm–coconut (PB15CB15) biodiesel separately on an unmodified direct injection diesel engine. Among 20% blends, palm–coconut combined blends reduced 0.54–1.85% NO_X emission with slightly improved BP. Compared to 30% palm and coconut blends, PB15CB15 provided improved BTE and emissions except NO_X. Arbab *et al.*[17] optimized the palm–coconut blending ratio by evaluating the combustion, performance and emission by palm–coconut blend (up to 20%) in a turbocharged and non-turbocharged unmodified diesel engine. They observed that combined palm–coconut blend provides superior performance and emission over individual palm biodiesel–diesel blend.

This experimental study examines the potential of using a combined blend of *Ceiba pentandra* and *Croton megalocarpus* biodiesel as a partial replacement for diesel fuel in a single-cylinder diesel engine. These biodiesels were blended based on the difference of cetane index between these two as the higher the cetane index, the better the combustion properties. ASTM D7467 suggests the blending of biodiesel with diesel from 6% to 20% (B6–B20). Biodiesel blends of up to 20% with diesel (B20) can be easily used in the existing diesel engines without the need for engine modification.[18] This study has particular relevance to South East Asian region where the potential exists for availability of both of these feedstocks and the establishment of economically viable application of biodiesels from these oils.

2. Materials and methodology

The crude of *C. pentandra* oil and *C. megalocarpus* oil were purchased from local markets. Highly pure analytical grade chemicals were chosen *e.g.* 96% pure H_2SO_4 (sulfuric acid), 99.8% pure CH_3OH (methanol), 85% pure KOH (potassium hydroxide) and 99% pure Na_2SO_4 (sodium sulfate) *etc.* The biodiesel production was carried out through a double jacketed batch glass reactor in laboratory scale with 2100 mL capacity.

2.1. Esterification process

As the crude *C. megalocarpus* and *C. pentandra* oil both contains the high acid value (more than 4 mg KOH per g), first pretreatment or esterification process was required to lower the FFA content of vegetable oil before going through the transesterification step. Acid catalyzed esterification of vegetable oil is recommended before transesterification if the acid value equal or more than 4 mg KOH per g.[19,20] The basic esterification reaction of a triglycerides is representing in the Fig. 1 where R represents small alkyl group and R^1 fatty acid chains.

In this process 1000 mL crude oil from both type was taken and preheat the oil at two different batch glass reactor at 60 °C to conduct the experiment. Methanol (CH_3OH) to oil molar ratio 12 : 1 (50% v/v oil) was maintained for *C. megalocarpus* and 18 : 1 (75% v/v oil) for *C. pentandra*. After preheating and adding methanol, 1% (v/v oil) of sulfuric acid (H_2SO_4) was added and maintain 60 °C reaction temperature for 3 h with 900 rpm stirring speed. After finishing the reaction, the reactants and products were poured into a separation funnel for 4 h to separate excess CH_3OH, H_2SO_4 and other impurities that were presented in upper layer of the separation funnel. Esterified lower layer products were collected and removed the dissolved methanol and water with the help of rotary evaporator (IKA, RV-10). 60 °C water bath temperature and 339 mbar vacuum

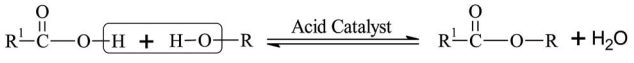


Fig. 1 Basic esterification reaction.

Published on 22 February 2016. Downloaded by University of Malaya on 08/03/2016 12:41:13.

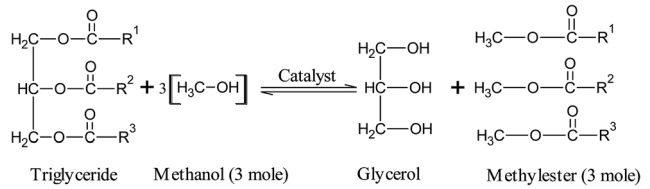


Fig. 2 Basic transesterification reaction.

pressure for methanol removal and then 70 °C temperature and 72 mbar vacuum pressure for water removal from the esterified product. This process was continued till confirming the absence of dissolved methanol and water into the esterified vegetable oil. By lowering the acid value less than 4 mg KOH per g through this process the esterified product becomes ready for transesterification.

2.2. Transesterification process

In this process the esterified *C. megalocarpus* and *C. pentandra* preheated at 60 °C in different batch glass reaction and 6 : 1 (25% v/v oil) methanol to oil molar ratio added. 1% (w/w oil) of potassium hydroxide (KOH) was mixed as catalyst with methanol before adding with the esterified oil. Then 60 °C reaction temperature was maintained for 2 h under 900 stirring speed. After finishing the reaction, the reactants and products were poured into a separation funnel for 12 h to separate glycerol from biodiesels. This time upper layer holds desire products or biodiesel (methyl ester) and lower layer contains impurities and glycerol. An ordinary outline of the transesterification reaction for fatty acid methyl ester (FAME) is showed in Fig. 2. Where R^1, R^2, R^3 represents fatty acid chains.[21]

2.3. Post treatment

After draining the lower layer out from separation funnel, upper layer or biodiesel layer were washed with 60 °C warm distilled water. The washing process was including sprays warm water in upper surface of the biodiesel, surface on separation funnel, shaking and stirred gently. The washing process was performed several times to properly remove the impurities from the produced methyl ester. Then the produced biodiesel was undergoing to the mechanical and chemical drying process. For mechanical drying, a rotary evaporator was used to evaporate methanol and water content from the biodiesel same condition like esterification process was applied for this removal process. For chemical drying, sodium sulfate anhydrous (Na_2SO_4) powder was used. Finally, the qualitative filter paper was used for separating the anhydrous from the biodiesel. The filtered and clean methyl ester is the desired biodiesel. It was observed that 96.5% yield and 97% yield was observed for *C. megalocarpus* and *C. pentandra* respectively.

Conventional biodiesel production technology associated with higher cost compared to per unit petroleum diesel production. About 60–75% biodiesel production cost is dependent on the sources.[22] Thus non-edible and second generation biodiesel sources have more popularity in the context of production cost and food security. Compared to Palm–Jatropha biodiesel production from low quality feedstocks (high free fatty acid and water content present) like Ceiba associated with higher processing cost at pretreatment and purification stage. By optimizing the production process and reaction condition, the production costing could be minimized about 1–5% compared to other well-known biodiesel production like Palm or Jatropha. Ceiba takes production cost around $0.36 per L whereas Jatropha takes $0.36 per L and *Calophyllum* $0.35 per L for a 5 kton capacity plant.[6]

3. Physicochemical property analysis

The physicochemical property of crude *C. megalocarpus* and *C. pentandra* oil were presented in Table 1. It was found that the acid value for both feedstocks are higher than 4 mg KOH per g. *C. pentandra* have the higher acid value (17.3 mg KOH per g)

Table 2 GC operating condition

Parameter	Setting value/condition
Column	0.32 mm × 30 m, 0.25 μm
Injection volume	1 μL
Carrier gas	Helium, 83 kPa
Injector	Split/splitless 1177, full EFC control
Temperature	250 °C
Linear velocity	24.4 cm s^{-1}
Split flow	100 mL min^{-1}
Column 2 flow	Helium at 1 mL min^{-1} constant flow
Oven	210 °C isothermal
Column temperature	60 °C for 2 min 10 °C min^{-1} to 200 °C 5 °C min^{-1} to 240 °C Hold 240 °C for 7 min 250 °C, FID, full EFC control

Table 1 Physicochemical property of crude *Croton megalocarpus* and *Ceiba pentandra* oil

Property	Unit	CCMO[c]	CCMO[a]	CCPO[c]	CCPO[b]
Density	kg m^{-3}	938.5	916.8	912.3	905.2
Kinematic viscosity@40 °C	mm^2 s^{-1}	44.5	49.4	33.5	34.45
Acid value	mg KOH per g	4.9	4.8	17.3	16.8
FFA	%	2.46	2.45	8.69	8.44
Flash point	°C	—	—	—	170.5

[a] Ref. 7 and 12. [b] Ref. 4. [c] Measured value.

 This journal is © The Royal Society of Chemistry 2016

Published on 22 February 2016. Downloaded by University of Malaya on 08/03/2016 12:41:13.

Table 3 Fatty acid composition of *Croton megalocarpus* and *Ceiba pentandra* biodiesel

FAME	Structure	Molecular weight	Composition CMB (wt%)	Composition CPB (wt%)
Methyl octanoate	C8:0	158.238	—	<0.1
Methyl decanoate	C10:0	186.291	—	<0.1
Methyl laurate	C12:0	214.344	—	<0.1
Methyl myristate	C14:0	242.398	<0.1	0.2
Methyl palmitate	C16:0	270.450	7.4	21.8
Methyl palmitoleate	C16:1	268.435	<0.1	0.5
Methyl heptadecanoate	C17:0	284.477	<0.1	0.1
Methyl stearate	C18:0	298.504	4.1	3.2
Methyl oleate	C18:1	296.488	12.2	22.6
Methyl linoleate	C18:2	294.472	71.2	40.7
Methyl linoelaidate	C18:2 isomar	294.472	—	4.1
Methyl linolenate	C18:3	292.456	3.4	3.8
Methyl γ-linolenate	C18:3	292.456	0.4	—
Methyl archidate	C20:0	326.557	—	0.7
Methyl icosanoate	C20:0 isomar	326.557	—	1.1
Methyl eicosenoate	C20:1	324.541	0.9	0.2
Methyl eicosadienoate	C20:2	322.525	<0.1	—
Methyl behenate	C22:0	354.610	—	0.6
Methyl erucate	C22:1	352.594	—	<0.1
Methyl lignocerate	C24:0	382.663	—	<0.1
Saturation			11.7%	28.1%
Mono-unsaturated			13.2%	23.4%
Poly-unsaturated			75.1%	48.6%
Unsaturated			88.3%	72%

than *C. megalocarpus* but lower density (912.3 kg m^{-3}) and viscosity (33.5 mm^2 s^{-1}) at 40 °C. Also the fatty acid composition of the crude *C. megalocarpus* and the *C. pentandra* oil is represented on the Table 1.

Fatty acid composition of the biodiesel sample was measured with the help of a GC (gas chromatographer). Agilent 7890 series, USA GC machine was used to measure the weight percentage of each FAME. Table 2 shows the GC operation condition for measuring the FAME composition.

It was observed that CPB contains the 28.1% saturated, 23.4% mono-unsaturated, and 48.6% poly-unsaturated methyl ester. Among them methyl oleate (C18:1) contains 22.6% and methyl linoleate (C18:2) contains 40.7%. On the other hand, CMB contains 11.7% saturated, 13.2% mono-unsaturated and 75.1% poly-unsaturated methyl ester. Among them majority portion (about 71.2%) was possessed by methyl linoleate (C18:2). It was observed that about 16.3% higher unsaturated FAME contains in CMB than CPB. The details FAEM contents are presented in Table 3.

Cetane Number (CN) were calculated from the percentage of fatty acid content, Iodine Value (IV), Saponification Number (SN) and using the eqn (1–3).[23]

$$\mathrm{SN} = \sum\left(\frac{560 \times A_i}{\mathrm{MW}_i}\right) \quad (1)$$

$$\mathrm{IV} = \sum\left(\frac{254 \times D \times A_i}{\mathrm{MW}_i}\right) \quad (2)$$

Table 4 List of equipment used for measuring the physicochemical properties[a]

Property	Equipment description	Manufacturer	Standard	Accuracy
Density	SVM 3000-automatic	Anton Paar, UK	ASTM D127	±0.1 kg m^{-3}
Kinematic viscosity	SVM 3000-automatic	Anton Paar, UK	ASTM D445	±0.35%
Viscosity index	SVM 3000-automatic	Anton Paar, UK	N/S	
Flash point	Pensky-martens flash point – automatic NPM 440	Normalab, France	ASTM D93	±0.1 °C
Cloud and pour point	Automatic NTL normalab NTE 450	Normalab, France	ASTM D2500	±0.1 °C
Cold filter plugging point	CFPP – automatic NTL 450	Normalab, France	ASTM D 6371	N/S
Acid value	G-20 Rondolino automated titration system	Mettler Toledo, Switzerland	D 664	±0.001 mg KOH per g
Calorific value	C2000 basic calorimeter – automatic	(IKA, UK)	ASTM D240	±0.1% MJ kg^{-1}
Oxidation stability, 110 °C	Metrohm 873 Rancimat	Metrohm, Switzerland		±0.01 hour

[a] N/S: Not specified.

Published on 22 February 2016. Downloaded by University of Malaya on 08/03/2016 12:41:13.

Table 5 Physicochemical properties of *C. megalocarpus* and *C. pentandra* biodiesel and their blends

		ASTM D975	ASTM 6751-08	Diesel	CMB[e] and CPB[e] blend						
Property	Unit	Diesel	Biodiesel	D100[e]	CMB	CMB20	CMB15CPB05	CMB10CPB10	CMB05CPB15	CPB20	CPB
Density@40 °C	kg m^{-3}	850[b]	880[b]	831.5	869.9	838.8	838.5	838.2	838.0	837.8	865.1
Kinematic viscosity@40 °C	mm^2 s^{-1}	1.3–4.1	1.9–6.0	3.9016	4.1287	3.9182	3.9297	3.9386	3.9515	3.9625	4.2927
Dynamic viscosity@40 °C	mPa s	—	—	3.2691	3.5917	3.2864	3.2949	3.3215	3.3115	3.3198	3.7137
Acid value	mg KOH per g	—	Max. 0.5	0.247	0.334	0.281	0.269	0.270	0.257	0.333	0.447
Iodine value	I_2 mg g^{-1}	—	—	—	115	109	107	89	93	103	107
Flash point	°C	60 to 80	93	79	190	88	85	83	84	86	157
Pour point	°C	−35	−15 to 16	−3	−5	—	—	—	—	—	2.8
Cloud point	°C	−20	−3 to 12	−2	−3	—	—	—	—	—	3
CFPP	°C	−25	Max. 5	−6	1	—	—	—	—	—	2
Calorific value	kJ kg^{-1}	42 000–46 000	—	45 802	39 951	44 397	44 349	44 302	44 255	44 208	39 001
Oxidation stability 110 °C	h	—	Min. 3	19.89	2.65	4.16	3.68	2.87	2.46	2.24	2.15
Cetane index	—	40–55[d]	Min. 47[d]	45.31[c]	42.40[a]	43.55[c]	44.02[c]	45.90[c]	46.26[c]	47.89[c]	50.36[a]
Carbon	wt%	84–87	77	87	76.88	—	—	—	—	—	76.45
Hydrogen	wt%	12–16	12	13	12.08	—	—	—	—	—	12.40
Oxygen	wt%	0–0.31	11	0	11.04	—	—	—	—	—	11.14

[a] Calculated from FAC. [b] Density@15 °C. [c] Calculated from ASTM 4737 method. [d] Cetane number. [e] Experimental result.

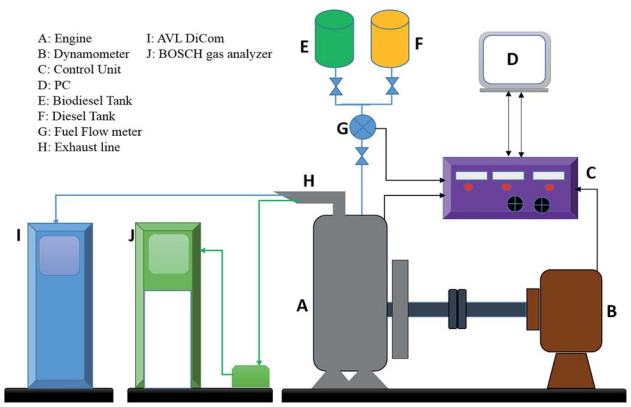


Fig. 3 Schematic of engine test bed.

$$CN = \left(46.3 + \left(\frac{5458}{SN}\right) - (0.225 \times IV)\right) \quad (3)$$

The physicochemical property of the produced biodiesel and different diesel–biodiesel blends (CMB20, CMB15CPB05, CMB10CPB10, CMB05CPB15, CPB20) were determined experimentally. The equipment's which were used for measuring the physicochemical property characterization are represented in the Table 4.

The comparison of measured result with diesel and biodiesel ASTM standard were represented in Table 5. All the properties were measured for three times and the average value was considered for getting more accurate result. Croton and Ceiba are of the Euphorbiaceae and Malvaceae family respectively due to which there are some physicochemical non-linearities between these two biodiesels. These non-linearities occurs mainly due to the type of their oil extraction sources (*i.e.* seeds). The seeds of these two shrub and tree are different in nature. Thus, they contain different type and percentage of saturated and unsaturated FAC in its crude oil. Thus, when these biodiesels are blended with diesel in different proportions, the physicochemical properties of the final blends changes according to the saturation level to each biodiesel. The degree of saturation of FAC of the final blends changes with the bleeding ratio. Thus, the cetane index of any blend increases when saturation percentage increases, whereas heating value increases when saturation percentage decreases of the final blends. Other properties also change in this manner.

4. Engine test setup

The experiment was performed in the heat engine laboratory of the Mechanical Engineering department of University of Malaya. To carry out the experiment a single-cylinder, four stroke, naturally aspirated, direct injection engine was used. A pump-line-nozzle injection system was integrated in the engine to inject fuel into the combustion chamber. An eddy current dynamometer was coupled with the engine for setting the load condition to the engine. Besides a laptop pc with Dynomax 2000 software and electronic interface was used to extract the engine performance data. A digital fuel flow meter was connected with the fuel flow line to measure the fuel consumption. BOSCH gas analyzer was used to measure the smoke opacity. AVL DiCom 4000 was connected to the engine exhaust line to measure the

 This journal is © The Royal Society of Chemistry 2016

Published on 22 February 2016. Downloaded by University of Malaya on 08/03/2016 12:41:13.

Table 6 Engine and dynamometer technical specification

Engine details	
Engine type	4 stroke DI diesel engine
Number of cylinders	One
Aspiration	Natural aspiration
Cylinder bore × stroke (mm)	92 × 96
Displacement (L)	0.638
Compression ratio	17.7
Maximum engine speed (rpm)	2400
Maximum power (kW)	7.7
Injection timing (deg.)	17° before TDC
Injection pressure (kg cm^{-2})	200
Power take off position	Flywheel side
Cooling system	Radiator cooling
Connecting rod length (mm)	149.5
Fuel system	Pump line nozzle injection
Dynamometer details	
Max. power	20 kW
Max. speed	10 000 rpm
Maximum torque	80 Nm
Water flow rate (maximum power)	14 L min^{-1}
Water pressure	23 lbf in^{-2}
Electricity	220 V, 50/60 Hz, 0.5 A
Dynamometer control unit	
Accuracy	0.10%
Precision	0.005% ± 1 digit
Weight measurement	Linear (load cell)
Speed measurement	Sensor
Operating temperature	Up to 70 °C
Operating voltage	230 VAC ± 10%, 50–60 Hz
Output	Dynomax 2000 software with PC interface

CO, CO_2, NO_X, and unburned HC emissions. All experiment was performed in full load condition and variable speed, speed variation form 1000 rpm to 2400 rpm. For a specific fuel, engine test was performed for three times in each condition and the average was considered as the result value of a specific condition. The engine test bed layout was presented in Fig. 3. More details technical data of the engine and dynamometer were shown on the Table 6.

4.1. Accuracy and uncertainty analysis

Instrumental accuracy and measuring uncertainty are kind of error during measuring data. Accuracy is the resolution of a measuring instrument which were provided by the manufacturer for a specific instrument. It indicates that how precisely the instrument can measure the value. Uncertainties in any experiments appear depending on the experimental conditions, instrument calibrations, observation, data input, test assembly *etc.*[24] Therefore, uncertainty analysis is a significant technique to validate the accuracy of the experimental results. A sample calculation for uncertainty and error analysis of brake power (BP) for diesel was presented in the Appendix "Tables 8" and "9", respectively. In this study percentage relative uncertainty was determined by the linearized approximation method of uncertainty. However, uncertainty calculation was performed based on the three test result of each parameter as well as for each condition.

Table 7 represents the other exhaust emission parameter measuring instruments with its accuracy and experimental uncertainty level. After calculating the individual uncertainty of measuring instrument, overall experimental uncertainty was computed by the eqn (4).

$$\text{Overall experimental uncertainty} = \sqrt{\sum (\text{uncertainty of each parameter})^2} \quad (4)$$

Overall experimental uncertainty = square root of [(uncertainty of BP)^2 + (uncertainty of BSFC)^2 + (uncertainty of BTE)^2 + (uncertainty of NO_X)^2 + (uncertainty of CO)^2 + (uncertainty of HC)^2 + (uncertainty of smoke)^2] = square root of [(±1.72)^2 + (±1.02)^2 + (±1.41)^2 + (±1.67)^2 + (±1.4)^2 + (±1.92)^2 + (±1.82)^2] = ±4.21%.

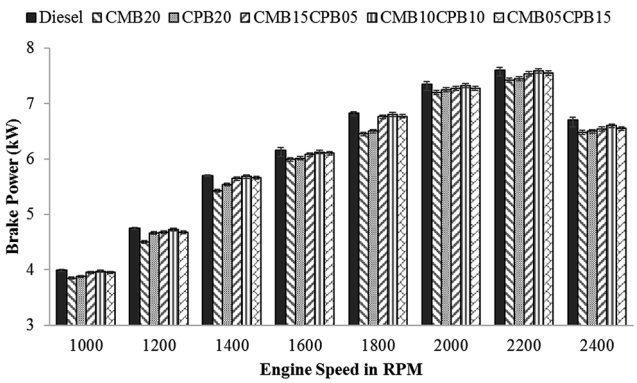


Fig. 4 Brake power *vs.* engine speed for full load condition.

Table 7 Gas analyzer specification

Equipment	Method	Measurement	Measuring range	Accuracy	% uncertainty
AVL DiCom 4000	Electrochemical detector	NO_X	0–5000 ppm vol	±1 ppm	±1.67%
	Non-dispersive infrared	HC	0–20 000 ppm vol	±1 ppm	±1.92%
	Non-dispersive infrared	CO	0–10% vol	±0.01% vol	±1.40%
	Non-dispersive infrared	CO_2	0–20% vol	0.1% vol	—
	Electrochemical detector	O_2	0–25% vol	0.01% vol	—
BOSCH RTM 430	Photodiode receiver	Smoke opacity	100%	±0.1%	±1.82%

Published on 22 February 2016. Downloaded by University of Malaya on 08/03/2016 12:41:13.

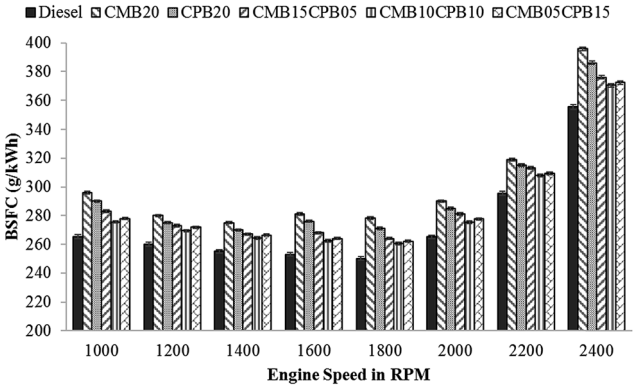


Fig. 5 BSFC *vs.* engine speed for full load condition.

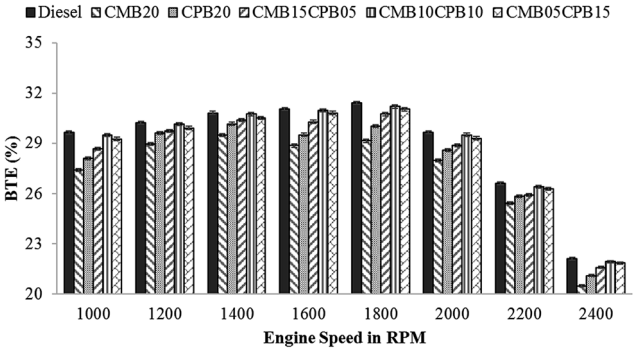


Fig. 6 BTE *vs.* engine speed for full load condition.

It was observed that the overall experimental uncertainty was less than 5% (95% confidence level), which was within the acceptable range.

5. Results and discussion

5.1. Performance analysis

Engine performance and fuel consumption were strongly governed by the physical and chemical properties of the fuel used. Engine performance parameters include BP, BSFC and BTE. This section represents the impact of 20% different biodiesel blends (CMB20, CMB15CPB05, CMB10CPB10, CMB05CPB15, and CPB20) of CMB and CPB in direct injection diesel engine at full throttle (100% load) condition with different engine speeds. The engine speed was varied for 1000 rpm to maximum 2400 rpm with an interval of 200 rpm.

5.1.1. BP. The engine performance mostly depends on fuel properties such as oxygen content, density, viscosity, calorific value *etc.* and fuel injection system.[15] Basically, these fuel property affects spray formation during fuel injection as well as it affects the combustion.[25] Fig. 4 demonstrates the effect on BP with the variation of speed at full load condition. It was clearly observed that for both diesel and biodiesel–diesel blend BP increases with the increasing of the engine speed up to rated speed 2200 rpm. At maximum speed (2400 rpm) power output decreased due to poor fuel atomization during combustion[26] and increase of piston cylinder frictional loses associated with higher engine speed.[27] Maximum BP was observed at 2200 rpm. The maximum BP were recorded 7.60, 7.45, 7.42, 7.54, 7.59 and 7.55 kW for diesel, CMB20, CPB20 CMB15CPB05, CMB10CPB10 and CMB05CPB15, respectively. BP output level was lower (about 1.09–3.7%) for biodiesel blends than petro diesel in all speeds. This can be attributed to combined effect of higher specific density, lower calorific value, higher viscosity and lower volatility (higher flash point compared to diesel) of biodiesels.[28] However, combined effect of this properties creates high injection in premixed region, poor fuel spray formation, incomplete combustion and high global fuel–air ratio equivalence ratio for lowering the BP of biodiesel blends than petro diesel.[19,29] This result, together with almost 12.07% lower calorific value of biodiesels can be attributed to the lower BP output than diesel. Among all the 20% biodiesel blends CMB10CPB10 showed the higher BP output at higher engine speed. This outcome may be attributed to the combined effect of the density and viscosity that diminish the inner spillage in the pump[30,31] and flash point that affects atomization or spray formation of fuel during combustion. Another reason could be the combined effect of additional oxygen content in biodiesels[17] and improvements of CN of combined blends. Accumulating lowest calorific value among all the combined blends, CPB20 demonstrated somewhat least BP. Addition of CPB with CMB improves the cetane index as well as the BP of the engine.

5.1.2. BSFC. BSFC is defined as fuel consumption per unit BP output for a specific fuel. Fuel properties *e.g.* density, viscosity and calorific value have significant influences on engine BSFC. Fig. 5 illustrates the BSFC in g kW^{-1} h^{-1} with variation of engine

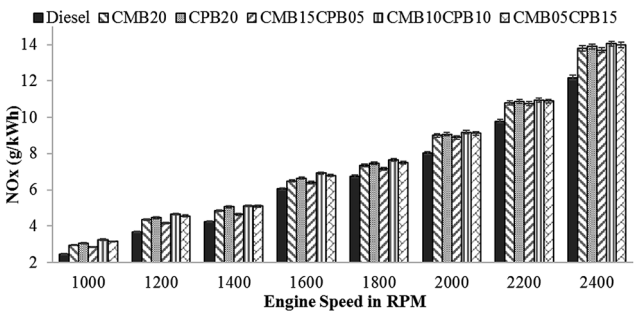


Fig. 7 NO_X emission *vs.* engine speed for full load condition.

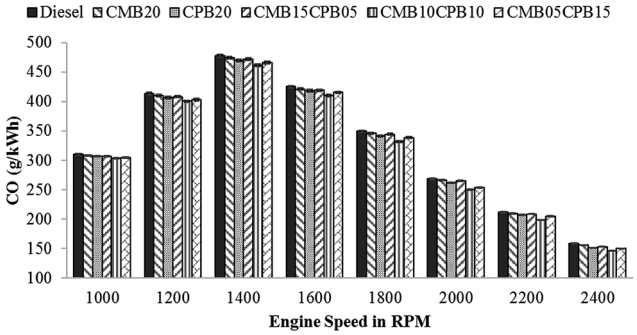


Fig. 8 CO emission *vs.* engine speed for full load condition.

This journal is © The Royal Society of Chemistry 2016

Published on 22 February 2016. Downloaded by University of Malaya on 08/03/2016 12:41:13.

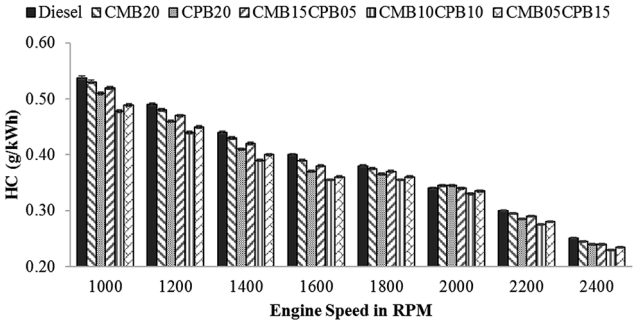


Fig. 9 HC emission *vs.* engine speed for full load condition.

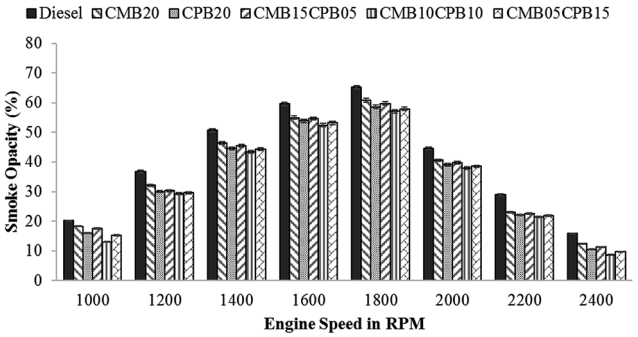


Fig. 10 Smoke opacity *vs.* engine speed for full load condition.

speed. The figure shows that BSFC of biodiesel blends is higher than that of petro diesel. This may be attributed to higher density and viscosity of biodiesel compared to diesel.[32] The figure also demonstrates that initially the BSFC for all fuels gradually decreased with increasing engine speed till 1800 rpm. This may be attributed to increased fuel atomization ratio, subsequently, the air–fuel equivalence ratio, which influences air and fuel mixing.[15] The lowest BSFC for diesel, CMB20, CPB20, CMB15CPB05, CMB10CPB10 and CMB05CPB15 were recorded 250.16, 278.23, 271.14, 264.05, 260.50 and 262.10 g kW^{-1} h^{-1}, respectively at 1800 rpm. BSFC gradually increased with the engine speed after 1800 rpm. Maximum BSFC for diesel, CMB20, CPB20, CMB15CPB05, CMB10CPB10 and CMB05CPB15 were recorded 355.62, 395.93, 386.00, 376.10, 370.53 and 372.41 g kW^{-1} h^{-1}, respectively at the maximum engine speed (2400 rpm). Volumetric efficiency decrease and increased frictional loss at higher speed might be the reason for this increase. In addition, BSFC increases with increasing engine speed and blend ratio of biodiesel.[26] Higher density and viscosity of biodiesel blends leads to higher mass flow rate in mechanically controlled pump-line-nozzle system as fuel is injected volumetrically affecting the fuel atomization.[33] Individual blends of CMB and CPB possess higher density and viscosity respectively, rather than combined blends which results in higher BSFC. With increasing amount of CPB in blend results in lower density but increased viscosity, which in turn increased surface tension of the blend. This resulted in a decrease in BSFC.

5.1.3. BTE. BTE is defined as break power of heat engine as a function of the heat input by the fuel. Fig. 6 shows the BTE for all tested diesel and biodiesel–diesel blends. The graphs demonstrated that BTE increased with engine speed up to 1800 rpm. This outcome is usually attributed for the highest BSFC was attained due to the consolidated impact of poor fuel atomization time and elevated piston-cylinder frictional force at this speed.[34] The height BTE value for diesel, CMB20, CPB20, CMB15CPB05, CMB10CPB10 and CMB05CPB15 were recorded 31.42%, 29.14%, 30.03%, 30.74%, 31.19% and 31.04, respectively. After 1800 rpm, BTE eventually decreased along with engine speed and achieved the lowest value at 2400 rpm for each of the investigated fuels. This results attributed to the higher fuel consumption for the increased engine speed. Compared to diesel maximum BTE of biodiesel–diesel blend were decreased by 0.50–5.97%. This changes due to the fuel variation were significant. BTE changed with the variety in BSFC and calorific value of the biodiesel. Though individual CMB20 possess higher calorific value that CPB20 as well as opposite for viscosity and CN, thus CMB20

Table 8 Uncertainty level calculation of BP, BSFC and BTE for diesel

	Three test			Max. and Min. value		Accuracy (±0.07 kW)			% uncertainty	
Power	Test 1 kW	Test 2 kW	Test 3 kW	Max. kW	Min. kW	Max. +0.07	Min. −0.07	Average	+	−
rpm	*A*	*B*	*C*	*D*	*E*	*F* = *D* + 0.03	*G* = *E* − 0.03	*H* = (*F* + *G*)/2	*I* = ((*F* − *H*)/*H*) × 100	*J* = ((*H* − *G*)/*H*) × 100
1000	3.98	3.98	4.00	4.00	3.98	4.07	3.91	3.99	2.01	−2.01
1200	4.74	4.75	4.76	4.76	4.74	4.83	4.67	4.75	1.68	−1.68
1400	5.69	5.70	5.71	5.71	5.69	5.78	5.62	5.70	1.40	−1.40
1600	6.09	6.16	6.20	6.20	6.09	6.27	6.02	6.14	2.03	−2.03
1800	6.83	6.80	6.85	6.85	6.8	6.92	6.73	6.82	1.39	−1.39
2000	7.29	7.40	7.37	7.40	7.29	7.47	7.22	7.34	1.70	−1.70
2200	7.55	7.61	7.65	7.65	7.55	7.72	7.48	7.60	1.58	−1.58
2400	6.64	6.71	6.76	6.76	6.64	6.83	6.57	6.70	1.94	−1.94
Uncertainty level of BP for diesel =									+1.72%	−1.72%
Similarly, uncertainty level of BSFC for diesel =									+1.02%	−1.02%
Uncertainty level of BTE for diesel =									+1.41%	−1.41%

Published on 22 February 2016. Downloaded by University of Malaya on 08/03/2016 12:41:13.

Table 9 Sample calculation of the error bar for power of diesel

	Test 1 kW	Test 2 kW	Test 3 kW	Average	Maximum value	Minimum value	+ve error	−ve error
rpm	*A*	*B*	*C*	*D* = (*A* + *B* + *C*)/3	*E*	*F*	*G* = *E* − *D*	*H* = *D* − *F*
1000	3.98	3.98	4	3.99	4.00	3.98	0.01	0.02
1200	4.74	4.75	4.76	4.75	4.76	4.74	0.01	0.02
1400	5.69	5.7	5.71	5.70	5.71	5.69	0.01	0.02
1600	6.09	6.16	6.2	6.15	6.20	6.09	0.05	0.11
1800	6.83	6.8	6.85	6.83	6.85	6.80	0.02	0.05
2000	7.29	7.4	7.37	7.35	7.40	7.29	0.05	0.11
2200	7.55	7.61	7.65	7.60	7.65	7.55	0.05	0.10
2400	6.64	6.71	6.76	6.70	6.76	6.64	0.06	0.12
Average error =							0.03	0.07

showed lower BTE than CPB20. On the other hand, combined blending provides better combination of density, viscosity as well as CN rather than individual biodiesel (CMB20 and CPB20) blends. Addition of higher percentage of CPB with CMB increases BTE and thus 10% combined blend of CMB and CPB provides the higher BTE as well as the lower BSFC among the biodiesel–biodiesel blends. Combustion phasing additionally impacts the energy conversion of heat energy to work. Quick injection of biodiesel together with high CN results in the early start of combustion (SOC).[35] Early SOC, raises pumping function and endorses heat decrease in the cycle.[31,33] This trend, collectively along with low heating value and higher density, viscosity, negatively impacts engine performance.[36,37]

5.2. Emission analysis

Emission parameter such as NO_x, CO, HC and smoke opacity were investigated throughout the experiments.

5.2.1. NO_x. NO_x emission mainly includes nitric oxide (NO) and nitrogen dioxide (NO_2) emission to the environment. NO is

Table 10 Sample of calculated cetane index for diesel (ASTM D4737-10)[a]

Distillation test result			Density, *D*@15 °C g mL^{-1}	DN (*D* − 0.85) g mL^{-1}	*B* ([e$^{(-3.5)(DN)}$] − 1)	T_{10N} (T_{10} − 215) °C	T_{50N} (T_{50} − 260) °C	T_{90N} (T_{90} − 310) °C
ASTM D86			D4052					
Test parameter	Unit	Result						
Initial boiling point	°C	177.5	0.8526	0.0026	−0.00906	17.7	29.2	39.3
5%	°C	216.8						
10%	°C	232.7						
20%	°C	252.7						
30%	°C	266.7						
40%	°C	278.0						
50%	°C	289.2						
60%	°C	301.4						
70%	°C	314.6						
80%	°C	329.7						
90%	°C	349.3						
95%	°C	367.1						
Final boiling point	°C	374.0						
Residue	%	1.5						
Recovery	%	98						
Loss	%	0.5						

$$CCI = 45.2 + (0.0892)(T_{10N}) + [0.131 + (0.901)(B)][T_{50N}] + [0.0523 - (0.420)(B)][T_{90N}] + [0.00049][(T_{10N})^2 - (T_{90N})^2] + (107)(B) + (60)(B)^2$$

Calculate cetane index for pure diesel = 45.31

[a] Where, CCI = calculated cetane index by four variable equation, *D* = density at 15 °C, g mL^{-1}, DN = *D* − 0.85, *B* = [e$^{(-3.5)(DN)}$] − 1, T_{10} = 10% recovery temperature, °C, $T_{10N} = T_{10} - 215$, T_{50} = 50% recovery temperature, °C, $T_{50N} = T_{50} - 260$, T_{90} = 90% recovery temperature, °C, $T_{90N} = T_{90} - 310$.

 This journal is © The Royal Society of Chemistry 2016

Published on 22 February 2016. Downloaded by University of Malaya on 08/03/2016 12:41:13.

the prevalent oxide delivered inside the engine cylinder. During combustion, atmospheric nitrogen (about 78.09% by volume) come into reaction and become the main source for NO_X emission for the internal combustion engine, this is treated as the thermal NO_X. Atmospheric tripled bonded nitrogen behaves as an inert gas but in high combustion temperature it splits up and undergoes with a series of reaction with oxygen and creates NO_2. This NO_X formation mechanism is known as Zeldovich mechanism. NO_X forms in prompt (Fenimore) mechanism because of the generation of hydrocarbon radicals *via* molecular unsaturation.[38,39] Fig. 7 demonstrate the NO_X emission for variable speed for full load. NO_X was gradually increasing with engine speed as the combustion temperature increase, with higher engine speed. The highest NO_X emission were observed for diesel, CMB20, CPB20, CMB15CPB05, CMB10CPB10 and CMB05CPB15 were recorded 12.18, 13.80, 13.90, 13.70, 14.05 and 13.99 g kW^{-1} h^{-1}, respectively at 2400 rpm. NO_X formation through the biodiesel blend is quite high due to 12–13% higher oxygen content in biodiesel, which provides high in-cylinder temperature for both premixed and diffusion combustion condition rather than diesel.[40] Together with higher CN, air surplus co-efficient, residence time and higher bulk modulus of elasticity can be ascribed as the reason for NO_X formation.[41,42] Bulk modulus of elasticity causes the early nozzle opening and advancement of the ignition, which increase global fuel–air equivalence.[43] Higher CN provides shorter ignition delay and higher oxygen content in biodiesel results higher combustion temperature. Because of the higher in-cylinder temperature during combustion CMB10CPB10 gives slightly higher and CMB15CPB05 provides relatively lower NO_X emission among the tested biodiesel blends.

5.2.2. CO. The partial combustion is the real cause of higher CO content in exhaust emissions, which caused by insufficient oxygen supply[44] during combustion. All this happens because of engine speed, air–fuel equivalence ratio, fuel pressure, fuel type and injection timing. Among them, ignition mixture because of lower air–fuel equivalence ratio can be considered as the main cause of CO emissions. Fig. 8 illustrates CO variation in different engine speeds at full load condition. Initially CO emission increased with increasing the engine speed ranging from 1000 rpm to 1400 rpm. This can be attributed to the lower air–fuel equivalence ratio, lower combustion temperature, poor atomization due to density, viscosity and flash point at low speed. On the other hand, at higher speed (after 1800 rpm) BSFC was found higher for biodiesel. With increasing of engine speed, higher air–fuel equivalence ratio, higher cylinder temperature and pressure was introduced during combustion, which ensures relatively better combustion and thus reduced the CO emission.[31,45] Overall biodiesel and biodiesel–diesel blends provides relatively lower CO emission in every speeds. This can be ascribed as higher oxygen content and higher CN of biodiesel, which shorting the ignition delay, thus provides better combustion and prevents less over-lean zones.[46] Maximum CO emission for diesel, CMB20, CPB20, CMB15CPB05, CMB10CPB10 and CMB05CPB15 were recorded 474.04, 469.97, 472.00, 461.13 and 466.51 g kW^{-1} h^{-1}, respectively at 1400 rpm. CO emission reduction for the biodiesel were obtained 1.09–5.21% with compare to diesel.

5.2.3. HC. The reasonable factors that creates the HC emission for petro diesel are fuel trapping in the crevice volume of combustion,[35] low temperature bulk quenching of oxidation reaction, locally over-lean or over-rich mixture, liquid wall filaments for excessive spray impingement and incomplete fuel evaporation.[47] The Fig. 9 illustrates the HC emission; it shows alike CO emission reduction. HC emission gradually decreases with increasing engine speed. It happens because of presence of oxygenate compounds in biodiesel. Also. This can be attributed to high in-cylinder temperature due to the high in cylinder pressure.[48] The maximum HC emission for diesel, CMB20, CPB20, CMB15CPB05, CMB10CPB10 and CMB05CPB15 were recorded as 0.537, 0.530, 0.513, 0.524, 0.484 and 0.496 g kW^{-1} h^{-1}, respectively at 1000 rpm. Compare with petro diesel, biodiesel blends and combined biodiesel blends reduces HC emission ranging from 1.48% to 8.38%. The biodiesel blend CMB10CPB10 gives the lowest HC emission.

5.2.4. Smoke opacity. Smoke emission refers to dark-black smoke or dry soot which is one of the principal source of particulate matter.[19] Smoke emission can be measured by the term smoke opacity. Fig. 10 illustrate the smoke opacity of diesel and biodiesel–diesel blend at variable engine speed. It shows smoke opacity of all blends of biodiesel is lower than petro diesel for all the engine speed due to oxygenated biodiesel fuel structure.[49] Inborn oxygen of biodiesel provides better combustion, thus lowering the smoke emissions than diesel.[41] Smoke emission gradually increases up to certain speed (in this case up to 1800 rpm), then gradually decreases up to maximum speed. The increases smoke opacity can be attributed to incomplete combustion of the hydrocarbon fuel and partial reaction of the carbon content in the liquid fuel[28] due to lower combustion temperature and poor atomization (due to density, viscosity and flash point) at low speed ranging from 1000 rpm to 1800 rpm. Maximum smoke opacity for diesel, CMB20, CPB20, CMB15CP05, CMB10CPB10, CMB05CPB15 were recorded 65.15%, 60.90%, 58.60%, 59.80%, 57.20% and 57.90%, respectively at 1800 rpm. After 1800 rpm, air–fuel equivalence ratio increases with engine speed and introduced higher combustion temperature which provides better burning of HC during combustion, thus decreased smoke opacity. However, tested biodiesel blends provides on an average 12.35–20.71% smoke emission reduction than petro diesel. Addition of CPB in CMB leads to an increase in viscosity and decrease in density, thus provides better BSFC and fuel atomization. Among all tested biodiesels and combined biodiesel blends, CMB10CPB10 provides slightly lower smoke opacity.

6. Conclusions

In this study biodiesel was produced from *C. megalocarpus* and *C. pentandra* feedstock and their physiochemical properties were examined. In addition, performance and emission characteristics of 20% biodiesel–diesel blend of CMB & CPB together with their combined blend were considered. These biodiesels

Published on 22 February 2016. Downloaded by University of Malaya on 08/03/2016 12:41:13.

were blended based on the difference of cetane index between these two as the higher the cetane index, the better the combustion properties. From the above experimental observation following conclusion can be drawn:

Compared to ordinary diesel, for all tested blends

• The average engine brake power was lower about 0.53% to 3.70%.

• BSFC were higher about 3.90% to 9.74% than that of diesel mainly owing to their lower heating value and higher density and viscosity.

• The BTE were slightly lower (about 0.50–5.97%).

• The average NO_X emission were 10.50% to 18.66% higher.

• The CO and HC emissions were reduced to an extent of 1.09–5.21% and 1.48–8.38%.

In conclusion, the lower brake power output from burning of *C. megalocarpus* biodiesel blends can be improved by the addition of *C. pentandra* biodiesel. At the same time, they slightly improve all emission except NO_X. Further research could be done by introducing some additives for improving the NO_X emission and the stability of the biodiesel blends.

Appendix

Nomenclature and abbreviations

BP	Brake power
BSFC	Brake specific fuel consumption
BTE	Brake thermal efficiency
CCMO	Crude *Croton megalocarpus* oil
CCPO	Crude *Ceiba pentandra* oil
CMB	Pure *Croton megalocarpus* biodiesel
CPB	Pure *Ceiba pentandra* biodiesel
CMB20	20% *Croton megalocarpus* biodiesel + 80% diesel
CPB20	20% *Ceiba pentandra* biodiesel + 80% diesel
CMB15CPB05	15% CMB + 05% CPB + 80% diesel
CMB10CPB10	10% CMB + 10% CPB + 80% diesel
CMB05CPB15	05% CMB + 15% CPB + 80% diesel
CO	Carbon monoxide
CO_2	Carbon dioxide
CP	Cloud point
CFPP	Cold filter plugging point
CN	Cetane number
FP	Flash point
FFA	Free fatty acid
FAC	Fatty acid composition
FTIR	Fourier transform infrared spectroscopy
FAME	Fatty acid methyl ester
GC	Gas chromatography
HC	Hydrocarbon
IV	Iodine value
NO_X	Oxides of nitrogen
NO	Nitric oxide
NO_2	Nitrogen dioxide
PP	Pour point
SN	Saponification number

Acknowledgements

The authors would like to thank the University of Malaya for financial support through High Impact Research grant titled: Development of Alternative and Renewable Energy Carrier (DAREC) having Grant Number UM.C/HIR/MOHE/ENG/60 and University Malaya Research Grant (UMRG) having Grant number RP016-2012B.

References

1 S. A. Shahir, H. H. Masjuki, M. A. Kalam, A. Imran, I. M. R. Fattah and A. Sanjid, *Renewable Sustainable Energy Rev.*, 2014, **32**, 379–395.
2 A. E. Atabani, T. M. I. Mahlia, H. H. Masjuki, I. A. Badruddin, H. W. Yussof, W. T. Chong and K. T. Lee, *Energy*, 2013, **58**, 296–304.
3 M. Tabatabaei, K. Karimi, I. S. Horváth and K. Rajeev, *Biofuel Res. J.*, 2015, **2**, 258–267.
4 A. S. Silitonga, H. C. Ong, T. M. I. Mahlia, H. H. Masjuki and W. T. Chong, *Fuel*, 2013, **108**, 855–858.
5 T. M. Y. Khan, A. E. Atabani, I. A. Badruddin, R. F. Ankalgi, T. K. M. Khan and A. Badarudin, *Ind. Crops Prod.*, 2015, **65**, 367–373.
6 H. Ong, A. Silitonga, H. Masjuki, T. Mahlia, W. Chong and M. Boosroh, *Energy Convers. Manage.*, 2013, **73**, 245–255.
7 G. Kafuku, M. K. Lam, J. Kansedo, K. T. Lee and M. Mbarawa, *Bioresour. Technol.*, 2010, **101**, 7000–7004.
8 H. C. Ong, H. H. Masjuki, T. M. I. Mahlia, A. S. Silitonga, W. T. Chong and T. Yusaf, *Energy*, 2014, **69**, 427–445.
9 A. Silitonga, H. Masjuki, T. Mahlia, H. C. Ong and W. Chong, *Energy Convers. Manage.*, 2013, **76**, 828–836.
10 S. Vedharaj, R. Vallinayagam, W. M. Yang, S. K. Chou, K. J. E. Chua and P. S. Lee, *Energy Convers. Manage.*, 2013, **75**, 773–779.
11 A. Bokhari, L. F. Chuah, Y. Suzana, A. Junaid, M. R. Shamsuddin and M. K. Teng, *Biofuel Res. J.*, 2015, **2**, 281–287.
12 G. Kafuku and M. Mbarawa, *Fuel*, 2010, **89**, 2556–2560.
13 B. Aliyu, D. Shitanda, S. Walker, B. Agnew, S. Masheiti and R. Atan, *Appl. Therm. Eng.*, 2011, **31**, 36–41.
14 B. R. Moser, *Renewable Energy*, 2016, **85**, 819–825.
15 M. Habibullah, I. Rizwanul Fattah, H. Masjuki and M. Kalam, *Energy Fuels*, 2015, **29**, 734–743.
16 M. Habibullah, H. H. Masjuki, M. A. Kalam, I. M. Rizwanul Fattah, A. M. Ashraful and H. M. Mobarak, *Energy Convers. Manage.*, 2014, **87**, 250–257.
17 M. I. Arbab, M. Varman, H. H. Masjuki, M. A. Kalam, S. Imtenan, H. Sajjad and I. M. Rizwanul Fattah, *Energy Convers. Manage.*, 2015, **90**, 111–120.
18 M. Kalam, H. Masjuki, M. Jayed and A. Liaquat, *Energy*, 2011, **36**, 397–402.
19 I. M. Rizwanul Fattah, M. A. Kalam, H. H. Masjuki and M. A. Wakil, *RSC Adv.*, 2014, **4**, 17787–17796.
20 I. M. Rizwanul Fattah, H. H. Masjuki, M. A. Kalam, M. A. Wakil, H. K. Rashedul and M. J. Abedin, *Ind. Crops Prod.*, 2014, **57**, 132–140.

 This journal is © The Royal Society of Chemistry 2016

Published on 22 February 2016. Downloaded by University of Malaya on 08/03/2016 12:41:13.

21 G. Moradi, M. Mohadesi, M. Ghanbari, M. Moradi, S. Hosseini and Y. Davoodbeygi, *Biofuel Res. J.*, 2015, **2**, 236–241.
22 A. Ruhul, M. Kalam, H. Masjuki, I. R. Fattah, S. Reham and M. Rashed, *RSC Adv.*, 2015, **5**, 101023–101044.
23 K. Krisnangkura, *J. Am. Oil Chem. Soc.*, 1986, **63**, 552–553.
24 M. A. Kalam and H. H. Masjuki, *Energy*, 2011, **36**, 3563–3571.
25 S. Murillo, J. Miguez, J. Porteiro, E. Granada and J. Moran, *Fuel*, 2007, **86**, 1765–1771.
26 I. R. Fattah, H. Masjuki, M. Kalam, M. Wakil, A. Ashraful and S. A. Shahir, *Energy Convers. Manage.*, 2014, **83**, 232–240.
27 M. A. Kalam, H. H. Masjuki, M. H. Jayed and A. M. Liaquat, *Energy*, 2011, **36**, 397–402.
28 H. How, H. Masjuki, M. Kalam, Y. Teoh and M. Abdullah, Effect of Injection Timing on Performance, Emission and Combustion Characteristics of a Common-Rail Diesel Engine Fuelled with Coconut Oil Methyl Ester, *SAE Technical Paper*, 2013.
29 Z. Chen, Z. Wu, J. Liu and C. Lee, *Energy Convers. Manage.*, 2014, **78**, 787–795.
30 E. Buyukkaya, S. Benli, S. Karaaslan and M. Guru, *Energy Convers. Manage.*, 2013, **69**, 41–48.
31 Ö. Can, *Energy Convers. Manage.*, 2014, **87**, 676–686.
32 M. I. Arbab, H. H. Masjuki, M. Varman, M. A. Kalam, H. Sajjad and S. Imtenan, *RSC Adv.*, 2014, **4**, 37122–37129.
33 F. Payri, J. M. Desantes and J. Benajes, in *Handbook of Clean Energy Systems*, John Wiley & Sons, Ltd, 2015.
34 S. Imtenan, H. Masjuki, M. Varman, I. R. Fattah, H. Sajjad and M. Arbab, *Energy Convers. Manage.*, 2015, **94**, 84–94.
35 S. Imtenan, H. Masjuki, M. Varman and I. R. Fattah, *RSC Adv.*, 2015, **5**, 17160–17170.
36 S. H. Park, J. Cha and C. S. Lee, *Appl. Energy*, 2012, **99**, 334–343.
37 P. Devan and N. Mahalakshmi, *Appl. Energy*, 2009, **86**, 675–680.
38 P. Benjumea, J. R. Agudelo and A. F. Agudelo, *Energy Fuels*, 2010, **25**, 77–85.
39 H. Sharon, K. Karuppasamy, D. S. Kumar and A. Sundaresan, *Renewable Energy*, 2012, **47**, 160–166.
40 D. Kannan, S. Pachamuthu, M. N. Nabi, J. E. Hustad and T. Løvås, *Energy Convers. Manage.*, 2012, **53**, 322–331.
41 S. Imtenan, H. H. Masjuki, M. Varman, M. A. Kalam, M. I. Arbab, H. Sajjad and S. M. Ashrafur Rahman, *Energy Convers. Manage.*, 2014, **83**, 149–158.
42 I. M. Rizwanul Fattah, M. H. Hassan, M. A. Kalam, A. E. Atabani and M. J. Abedin, *J. Cleaner Prod.*, 2014, **79**, 82–90.
43 A. L. Boehman, D. Morris, J. Szybist and E. Esen, *Energy Fuels*, 2004, **18**, 1877–1882.
44 S. S. Reham, M. A. Kalam, I. Shancita, H. H. Masjuki, I. M. Rizwanul Fattah and A. M. Ruhul, *Renewable Sustainable Energy Rev.*, 2015, **52**, 1566–1579.
45 C. Sayin, *Fuel*, 2010, **89**, 3410–3415.
46 A. Sanjid, H. H. Masjuki, M. A. Kalam, S. M. A. Rahman, M. J. Abedin, M. I. Reza and H. Sajjad, *Procedia Eng.*, 2014, **90**, 397–402.
47 J. B. Heywood, *Internal combustion engine fundamentals*, Mcgraw-hill, New York, 1988.
48 I. Shancita, H. Masjuki, M. Kalam, S. Reham, A. Ruhul and I. Monirul, *RSC Adv.*, 2016, **6**, 8198–8210.
49 H. J. Curran, E. M. Fisher, P.-A. Glaude, N. M. Marinov, W. Pitz, C. Westbrook, D. Layton, P. F. Flynn, R. P. Durrett and A. Zur Loye, *Detailed chemical kinetic modeling of diesel combustion with oxygenated fuels, Report 0148–7191, SAE Technical Paper*, 2001.

View publication stats